Canadian Conference - Pacific Conference on Earthquake Engineering 2023

Vancouver, British Columbia

June 25th – June 30th, 2023

Quantifying Variability in the Collapse Risk of Tall Non-Ductile Reinforced Concrete Shear Wall Buildings

Preetish Kakoty[1*], Carlos Molina Hutt[2], and Kenneth J Elwood[3]

[1]PhD Candidate, Department of Civil Engineering, University of British Columbia, Vancouver, BC
[2]Assistant Professor, Department of Civil Engineering, University of British Columbia, Vancouver, BC
[3]Professor, Department of Civil and Environmental Engineering, University of Auckland, Auckland, NZ
[*]preetish.kakoty@ubc.ca (Corresponding Author)

ABSTRACT

Since the late 1950s, tall reinforced concrete shear wall (RCSW) buildings have been predominant (~80% of all tall buildings) in the Metro Vancouver region of southwestern British Columbia. In the mid-1980s, a number of factors, including ductility and other detailing requirements, improved the design and construction practice of these buildings. The new design requirements highlighted the vulnerabilities of RCSW buildings constructed prior to the 1980s. These vulnerabilities include the use of thin walls (~200 mm) with a single layer of reinforcement, the absence of boundary zones, and low wall areas relative to the floor area. This study evaluates the collapse risk tall pre-1980 RCSW buildings, which represent close to 30% of all tall buildings in Metro Vancouver, by developing and analyzing 3D fiber-based numerical models of representative archetypes. The archetypes are generated using a machine learning based predictive model that leverages an existing detailed database of this taxonomy of buildings. The database includes information such as building floor area, wall layout, reinforcement details, etc. for approximately 200 buildings. To streamline the analysis framework, a workflow is developed to generate the nonlinear structural analysis models automatically in OpenSeesPy, using outputs from the archetype predictive model. A multiple stripe analysis is carried out at a range of hazard levels to characterize the collapse risk of each archetype building. Ground motion records were selected at each hazard level per the requirements of the 2015 National Building Code of Canada representing three unique tectonic regimes. The results of the study are used to investigate the variability in the collapse risk of this taxonomy of buildings. The impact of unique structural features (e.g., wall layout, material properties, etc.) in the anticipated collapse risk of these structures is also explored. The results indicate that while the annualized collapse risk can vary significantly from building to building, the risk is, on average, five times higher than that of modern RCSW buildings.

Keywords: Non-Ductile Reinforced Concrete Shear Wall Buildings, Collapse Risk, Seismic Risk, OpenSeesPy

INTRODUCTION

One of the key challenges in earthquake engineering is addressing the seismic risk posed by existing buildings, especially the ones constructed prior to the advent of modern building codes [1, 2]. Reinforced concrete shear wall (RCSW) buildings have been commonly used as the lateral force resisting system in regions of high seismicity around the world. For instance, RCSWs are predominant in tall building construction in the Metro Vancouver region. Tall RCSW buildings in this region experienced a surge in construction from the mid-1960s to early 1980s, and then again post-1990s [3]. Significant changes were introduced in the design and construction practices of tall RCSW buildings during the mid-1980s, resulting in two distinct categories in terms of expected seismic performance, buildings built prior to mid-1980s and those built after that. The latter are perceived to have significantly better seismic performance. Two major design changes, as explained by Adebar et al. [3], include significant new ductility requirements for flexural walls introduced by the 1984 edition of CSA A23.3 [4], coupled with increased seismic demands in the 1985 edition of the National Building Code of Canada (NBCC) [5]. Modern shear wall buildings are generally expected to perform satisfactorily, in terms of life safety, under earthquake loading. However, older constructions are vulnerable to brittle failure mechanisms [6–8]. Older RCSW buildings in other geographical regions have been observed to suffer significant damage and, in some cases, collapse in past earthquakes, e.g., the 2010 Maule earthquake [8] and the 2011 Christchurch earthquake [9]. The poor performance of these older RCSW buildings can be attributed to the poor configuration of the structural system, and the brittle behavior of thin walls, which are also found in Metro Vancouver.

Development of detailed building inventories is a critical step towards understanding and assessing seismic risk. Such databases serve as the basis to quantify the risk posed by existing buildings. This paper assesses the collapse risk of a series of archetype pre-1980 tall RCSW buildings, which are developed by leveraging a database, developed by Yathon et al. [6], of about 350 such buildings located in City of Vancouver. This database used existing databases of buildings (i.e., Onur et al. (2005) and Emporis (2013)), augmented with structural drawings sets from the City of Vancouver archives to collect detailed building information. The inventory includes general building information (e.g., construction year, number of stories, floor area, shear wall area, etc.), critical column details (e.g., dimensions, column reinforcement, position, etc.), and wall details (e.g., dimensions, wall attachments, wall reinforcement, etc.).

Three-dimensional fiber-based nonlinear structural analysis models are developed for all archetype buildings to simulate seismic response under earthquake loading. The fiber-based models considering bar buckling following concrete crushing under compressive strains and bar rupture under tensile strains, consistent with past observations of failure mechanisms in these walls [7–10]. Observations of this brittle failure mechanism highlight key parameters such as high axial load, lack of detailing, low reinforcement ratio, etc. as they correlate to damage in these non-ductile shear walls. Impacts of axial load ratios on the drift capacities of the shear walls are considered using empirical data from a large set of experimental test results [11]. These analyses are utilized to quantify collapse risk of this inventory of buildings and examine variations of their collapse risk. This paper illustrates the methodology for selection and development of structural analysis models of archetype RCSW buildings, and highlights the variation in their collapse risk.

Seismic performance of this taxonomy of buildings will have a significant impact on the regional risk in the City of Vancouver due to its high concentration in the downtown area, particularly the West End neighborhood. The results of this study will provide insights into the variation in seismic performance and associated risk metrics in this taxonomy of buildings. The results of this work will also enable the development of regional seismic risk models with higher resolution. Particularly, when compared to conventional regional risk assessment methods that employ generic fragility and vulnerability functions to characterize seismic damage and the associated impacts on the community. In these conventional risk models, tall non-ductile reinforced concrete buildings, greater than 8 stories, fall under the same taxonomy and hence seismic risk metrics will be quantified using the same functions making no significant distinction between a 10 vs 30 story building, and not recognizing that unique building features will influence anticipated seismic performance.

NUMERICAL MODELS OF NON-DUCTILE REINFORCED CONCRETE SHEAR WALL BUILDINGS

Archetype selection

An existing detailed inventory [6] of about 350 pre-1980 non-ductile reinforced concrete shear wall buildings in Vancouver of seven or more stories was used to inform the creation of archetype buildings. Yathon et al. [6] identified key deficiencies within the inventory, including the use of thin walls (~200 mm), single layer of steel reinforcement, lack of boundary zone detailing, vertical irregularity, etc. This study evaluates a total of five 10-story archetypes that are informed by trends identified in the building inventory. Numerical models are generated for each archetype to conduct nonlinear time history analyses and quantify collapse risk. Random forest regression models are used in identifying the archetypes, the detail of which is forthcoming [12]. All the selected archetypes consist of 200 mm shear walls with a single layer of reinforcement, and with no detailing in the boundary zone. Other parameters, such as those listed in Table 1, are based on the trends observed in the existing database [6]. For instance, the median floor area of 10-story buildings in the database is 398 m^2, and ranges from 254 m^2 at the 10th percentile to 560 m^2 at the 90th percentile. Similarly the median shear wall area, normalized by the floor area, in the long building direction is 1%, and ranges from 0.51% at the 10th percentile to 2.16% at the 90th percentile. Table 1 summarizes the key parameters of the five 10-story archetypes selected for this study.

Table 1. Structural features of selected archetype buildings.

Archetype ID	Fundamental Period (s)			Floor Area (m^2)	Aspect Ratio	Shear Wall Area (%)	
	1st Mode	2nd Mode	3rd Mode			Longer Direction	Shorter Direction
1	1.13	0.57	0.35	554	2.24	1.78	0.7
2	0.83	0.79	0.49	675	1.09	0.99	0.87
3	0.75	0.57	0.56	483	1.49	1.33	1.16
4	0.76	0.58	0.56	411	2.39	1.15	1.13
5	0.96	0.66	0.63	321	1.16	1.63	1.35

Modeling Assumptions

Numerous studies have developed numerical models to simulate the response of tall RCSW buildings, both modern and older ones, to earthquake ground motions. Most commonly, fiber-based beam-column elements have been used to model shear walls [13–16]. This fiber-based approach utilizes uniaxial material models to capture nonlinear hysteretic axial stress-strain characteristics in the wall cross-section to capture its axial-flexural response. Shear behavior is typically modeled by means of linear spring elements. While the shear-flexural response in these models is generally decoupled, multilayered shell elements have been used in other studies [17] to capture shear-flexure interaction. This study, however, uses the fiber-based modeling approach because most of the walls in the buildings considered are flexure dominated [6]. Furthermore, this approach allows for the development of models within an automated workflow and can accurately simulate the cyclic response of walls, considering strength and stiffness degradation, in a computationally efficient manner.

Pugh et al. [15] used a collection of post-earthquake reconnaissance reports and experimental results to identify that compression damage in the boundary elements and web crushing failure modes are predominant modes of failure in reinforced concrete shear walls. In their work, they adopted a force-based distributed plasticity fiber-based beam-column element to develop computationally efficient numerical models that capture strength loss due to these dominant failure modes. More recently, Marafi et al. [14] utilized displacement-based elements to model walls to "achieve accurate and mesh-objective simulation of wall response". Gogus et al. [13] modeled the walls using displacement-based distributed plasticity beam-column elements, supplemented with shear and rotational springs to simulate shear flexibility and deformation due to bar pullout at the base of the wall. Loss of lateral strength was not explicitly modeled in their study; instead, simulation data were post processed to determine the onset of collapse. Collapse criteria included: (1) exceedance of 0.01 compressive strain in unconfined concrete or 0.06 in confined concrete, (2) exceedance of 0.05 steel tensile strain, which was defined as less than the fracture strain under monotonic loading to account for low-cycle fatigue, (3) exceedance of 0.015 shear strain, and (4) exceedance of 5 % story drift ratios, which was intended to represent failure of the gravity load-resisting system. These studies focused on assessing seismic performance of modern reinforced concrete shear wall buildings designed following modern building code requirements, which ensure sufficient flexural strength and stiffness, with the goal of developing favorable plastic behavior under earthquake loading.

By contrast, older non-ductile reinforced concrete shear walls are expected to exhibit brittle failure due to a lack of confinement and inadequate detailing. Empirical evidence gathered from 36 damaged buildings in the aftermath of the 2010 Chile earthquake indicated that high axial load ratios ($\geq 10\% \, f_c' A_g$, where f_c' is the compressive strength of concrete and A_g is the gross area of the section) were the most significant factor in inducing failure at the bottom of shear walls [7], with compounding vulnerabilities such as the lack of detailing in the boundary zones, high aspect ratios and wall slenderness. Analysis of a large dataset of experimental test results of non-ductile shear walls also supports the notion that axial failure tends to precede lateral failure under higher axial load ratios, leading to concrete crushing followed by bar buckling at higher compressive strains [11]. In addition to these deficiencies, many of these buildings have significant vertical irregularities, which can further exacerbate the damage caused by earthquakes due to high stress concentrations at the locations of vertical irregularity.

Although both force-based and displacement-based element formulations are used in the literature, this study adopts a force-based formulation with fiber-based beam column elements in OpenSeesPy [18]. This force-based formulation provides good estimates of response with better computational efficiency than the displacement-based formulation. While in the displacement-based formulation, accuracy can be improved by increasing the number of elements [19], this can lead to significant increases in computational demand. In the force-based formulation, better accuracy can be achieved by optimizing the number of integration points along the element.

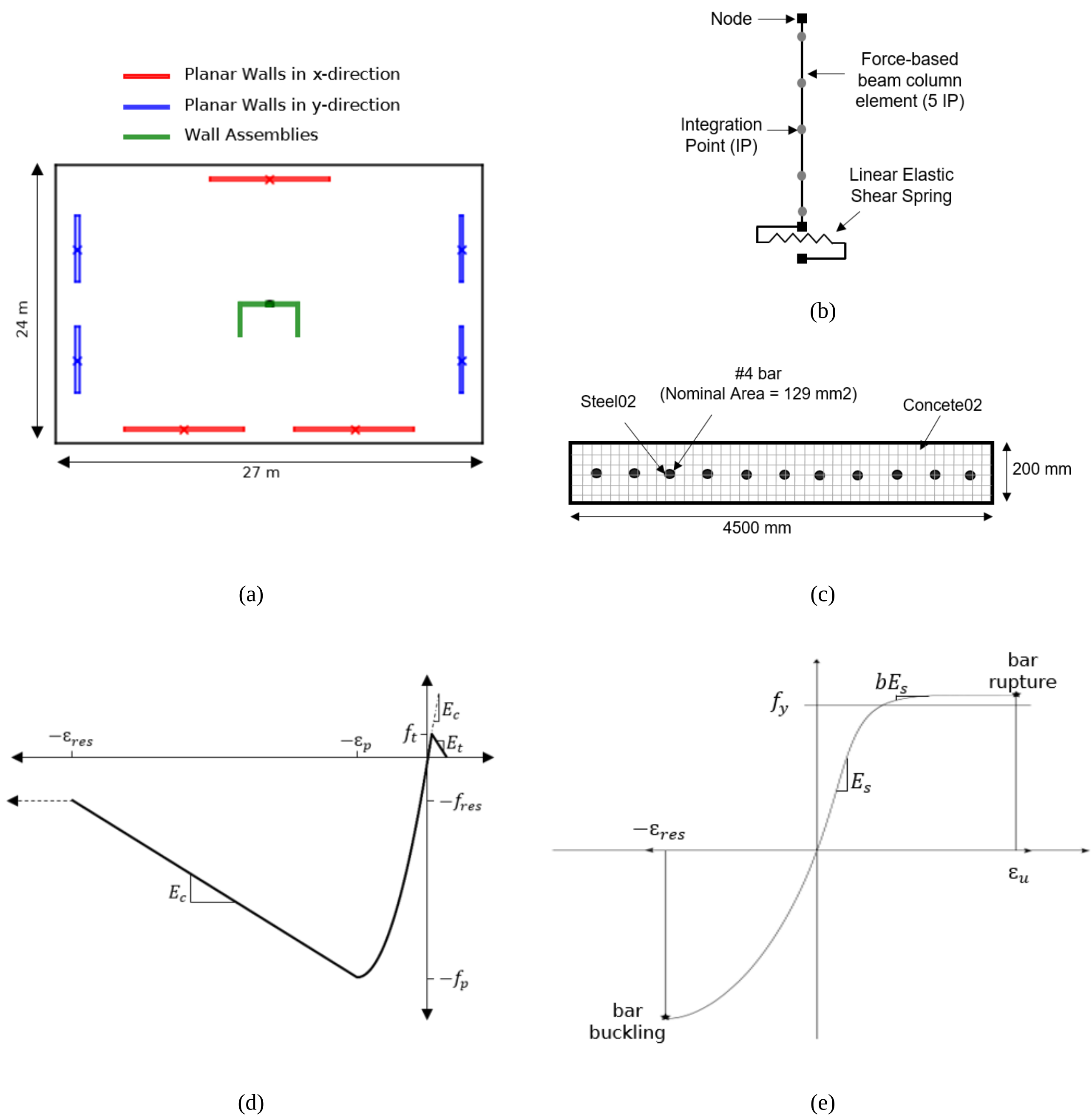

Figure 1. Schematic of (a) floorplan of Archetype #1 from Table (1); (b) OpenSeesPy model illustrating force-based elements; (c) cross-section of a sample wall; and stress-strain relationship of (d) concrete fiber; and (e) reinforcing steel fiber

Concrete02 and *Steel02* material models in OpenSeesPy are used to simulate the cyclic response of concrete and steel materials respectively. *Concrete02* [20] follows the Hognestad [21] stress-strain relationship for pre-peak response, and a linear post-peak degradation until it reaches a residual capacity corresponding to the residual strain level (ε_{res}), as shown in Figure 1d. *Steel02* follows a stress-strain relationship defined by Menegotto and Pinto [22], as shown in Fig 1e. To simulate the effects of bar buckling and rupture, at extremes of compressive and tensile strains, a *MinMax* wrapper is used to force the steel material to loose capacity at ε_{res} for buckling and at ε_u for rupture respectively, annotated schematically in Figure 1e. This is critical to account for simultaneous loss of strength of concrete and longitudinal bar buckling, which is a common failure type observed in the walls of interest [7–10]. Pugh et al. [15] showed that while loss of strength for concrete can be captured well, deformation is localized in the failing elements resulting in “mesh-dependence”. To mitigate such “mesh-dependent” results, Pugh et al.

[15] recommended regularizing material models by defining post-peak response as a function of a mesh-dependent characteristic length (L_E) and the expected material yield crushing energy (G_f). Specifically for the concrete material, regularized strain at the onset of residual compressive strength (ε_{res}) is computed as shown in Eq. (1).

$$\varepsilon_{res} = \frac{2G_f}{(\beta + 1)f_p L_E} + \varepsilon_p \frac{\beta + 1}{2} \tag{1}$$

Where G_f is the concrete crushing energy, β is the percentage of f_p corresponding to the residual compressive strength, L_E is the length over which softening occurs in the model, and ε_p.is the strain of the concrete material at peak compressive strength.

Calibration of Material Models

Four test specimens with varying axial load ratios and wall thickness tested at the University of Auckland [23] were used to validate the modelling approach of the non-ductile reinforced concrete shear walls and calibrate material model properties. Figure 2 shows the force-deformation response of a specimen with a 200 mm thick wall and 10% axial load ratio, against the results of an analytical model. The full scale wall specimens were designed to represent typical flexure-controlled reinforced concrete shear walls consistent with construction practices from the 1950s to the 1970s in New Zealand. These walls have similar properties to the ones in non-ductile RCSW buildings in Vancouver, i.e. thin walls, single layer of reinforcement, lack of boundary zone, etc. The wall specimen have lengths and heights of 1920 mm and 3840 mm, respectively. A distributed reinforcement ratio of 0.25% is adopted in all walls, which represents the average distributed reinforcement ratio for typical older walls [24]. The modeling approach previously described was utilized to simulate the cyclic response of the wall tests.

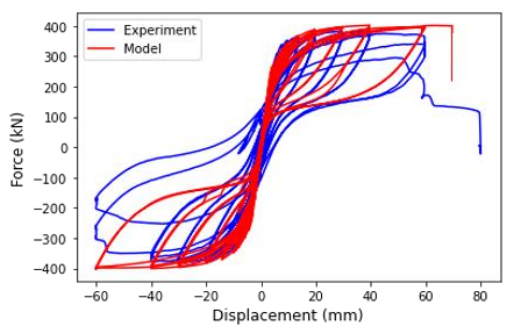

Figure 2. Force-displacement response of a 200 mm thick wall specimen, singly reinforced and with 10% axial load ratio (blue) plotted against the results of an equivalent numerical model (red).

As described by Zhang [23], the wall specimens were subjected to cyclic loading with increasing level of displacement until failure. At failure, concrete spalling usually triggered buckling of reinforcing steel resulting in immediate loss of lateral strength. Concrete spalling in the wall specimens were observed separately in the extreme ends and in the middle as an indication of initiation of strength degradation and significant loss of lateral strength, respectively. The behavior of the wall specimens was dominated by one or two horizontal cracks at the bottom of the wall panel initiating concrete spalling in the boundary and exposing the vertical reinforcement, followed by buckling due to lack of confinement. Wall specimens with low axial load ratio (3.5%) resulted in gradual lateral strength degradation while carrying the axial load until failure (~2% drift ratio). Wall specimens with higher axial load ratio (10%) resulted in axial failure, at lower drift ratios (~1.5%), with concrete crushing over the length of the wall.

Lower drift capacities for these walls at higher axial load ratios have been corroborated by studies in the past [11, 25]. Test results from past research indicate very low drift capacity (~1%) at failure in poorly detailed walls [25]. A study by Abdullah and Wallace [11] analyzed results from a large number of tests and proposed an empirical relationship to quantify drift capacity of the walls as a function of slenderness, level of detailing, and axial load ratio, as shown in Eq. (2). This study also found that axial and lateral failure occurs simultaneously at lower levels of drift, in poorly detailed walls with higher axial load ratios ($\geq 10\%$). Eq. (2) shows the empirical relationship between mean drift capacity at axial failure (Δ_a/h_w) as a function of the slenderness parameter (λ_b) and axial load ratio $(P/A_g f_c')$. Figure 3 illustrates the drift capacities, as estimated from Eq. (2), of wall sections in the archetypes evaluated in this study.

$$\frac{\Delta_a}{h_w}(\%) = 3.65 - \left(\frac{\lambda_b}{30}\right) - \left(3.5\frac{P}{A_g f_c'}\right) \geq 0.8\% \tag{2}$$

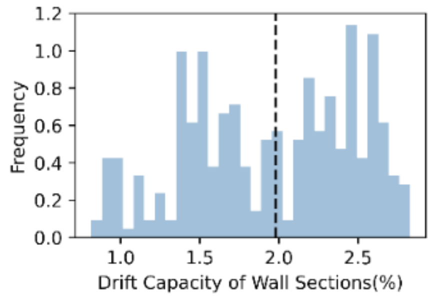

Figure 3: Frequency of drift capacities, as estimated from Eq. (2), of wall sections in the selected archetypes, the vertical black dashed line indicate the median.

COLLAPSE RISK ASSESSMENT

Methodology

Multiple stripe analysis (MSA) [26] is used in this study to evaluate the probability of collapse at a range of hazard levels. MSA involves conducting nonlinear time history analysis at selected intensity measure "stripes" (representing distinct hazard levels) with ground motions selected and scaled to be hazard-consistent. The steps involved in the collapse assessment methodology are as follows:

i. ***Structural Analysis:*** Nonlinear time history analyses of each archetype building model are carried out at four hazard levels with return periods of 100, 475, 975, and 2475-year. At each hazard level, a total of 33 ground motions are selected, 11 each from crustal, inslab, and interface earthquake sources. Ground motions are selected as per the framework prescribed in the National Building Code of Canada [27]. Collapse cases are identified at each hazard level and the fraction of collapse cases at each hazard level is used to develop a collapse fragility.

ii. ***Collapse Identification:*** Collapse is assumed to occur when the lateral displacement of the archetype building models causes dynamic instability, due to loss of strength caused by excessive lateral and/or axial demand. In addition to global failure due to large lateral displacements, partial collapse could occur due to the failure of the shear walls usually triggered by concrete crushing followed by reinforcing bar buckling. This is simulated by complete loss of strength in the steel material model at a compressive strain level corresponding to onset of residual strength of the concrete material. Furthermore, to account for non-simulated collapse, a drift capacity of 2% is assumed based on the results previously shown in Figure 3.

iii. ***Develop Collapse Fragility:*** The fraction of collapse cases, or probability of collapse, is evaluated at each hazard level and corresponding intensity measure. A lognormal cumulative distribution, referred to as a collapse fragility, is fitted the resulting probabilities of collapse by using the maximum likelihood estimator [28]. Figure 4 shows multiple stripe analysis of one 10-story archetype building model, and the collapse fragility function that summarizes probability of collapse as a function of spectral acceleration at the fundamental period of the building.

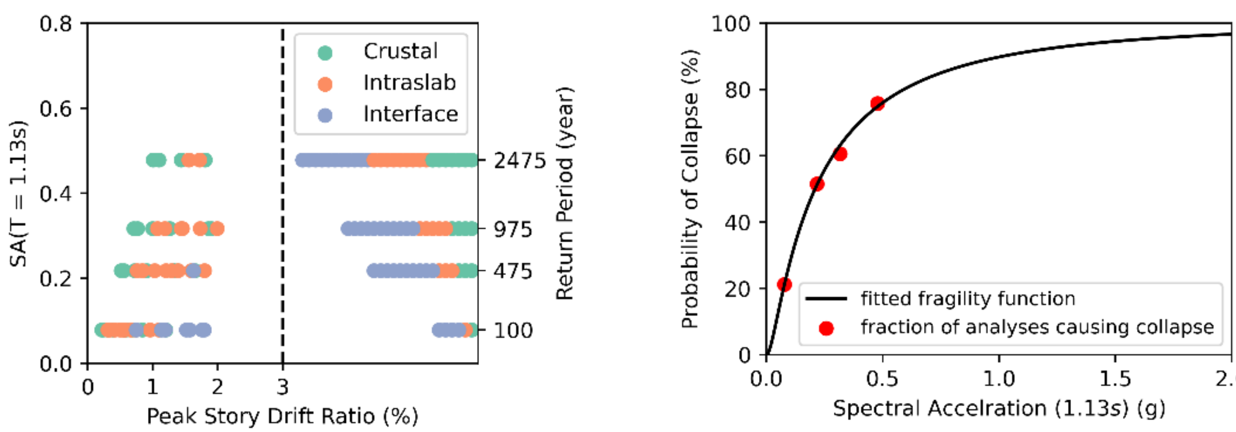

(a) (b)

Figure 4: Multiple stripe analysis results of a sample 10-story archetype to (a) identify collapse cases from nonlinear time history analysis (dots on the right side of the dashed line indicate collapse cases); and derive (b) fitted lognormal collapse fragility function for the given archetype.

Annualized Collapse Risk

Annualized collapse risk estimates are widely used in seismic risk management. This metric is calculated by integrating the a collapse fragility with corresponding seismic hazard curve at the site of interest. Annualized collapse risk estimates are also used to benchmark against modern collapse risk targets in modern seismic design standards. For instance, U.S. building codes target a collapse risk of 1% in 50 years. Eq. (3) illustrates the calculations involved in calculating the annualized collapse risk (λ_c).

$$\lambda_c = \int_0^\infty P(C|IM = im) \left|\frac{d\lambda(IM)}{dIM}\right| dIM \tag{3}$$

Where $P(C|IM = im)$ is the conditional probability of collapse for a given intensity measure, im, $\frac{d\lambda(IM)}{dIM}$ is the slope of the seismic hazard curve at the site, and dIM represents the differential of intensity measure in the hazard curve.

The annualized collapse risk is used to calculate the 50-year collapse risk by assuming that collapse occurrence follows a Poisson distribution. Figure 5 shows the probability of collapse in 50 years, as well as annualized collapse risk of the five 10-story archetypes evaluated in this study. The probability of collapse in 50 years in these older non-ductile RCSW buildings ranges from 26.6% to 35.3% as shown in Figure 5. Although building codes in Canada do not have an explicit collapse risk target, past studies have suggested that modern Canadian buildings have a similar collapse risk to that targeted by US building standards [17, 29]. By contrast, these older non-ductile RCSW buildings have drastically higher collapse risks, up to thirty-five times the US target of 1% in 50 years. Non-ductile RC frame structures in California are reported to have probability of collapse in 50 years in the range of 21% to 50% [30], in the same range as the non-ductile RCSW archetypes in this study.

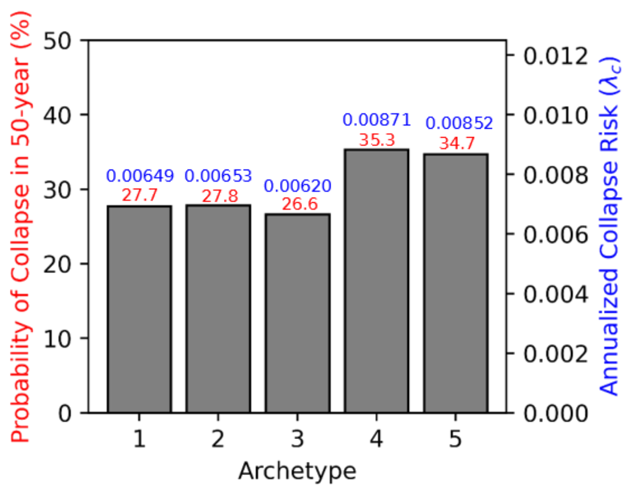

Figure 5: Estimated probability of collapse in 50-year and annualized collapse risk (λ_c) for of the five 10-story archetypes

Variability in Collapse Risk

Figure 6 illustrates collapse fragility functions for the five selected 10-story archetypes. The probability of collapse is shown as a function of return period, in lieu of spectral acceleration at fundamental period of vibration, to enable a direct comparison of the resulting collapse fragilities across archetypes with distinct periods of vibration. While there is variation across the resulting collapse fragilities, the 50% collapse probabilities are associated with return periods ranging from ~300 to ~500 years. Furthermore, 10% probability of collapse, denoted by the dashed black line in Figure 6, corresponds to return periods in the range of ~40 to ~60 years. By contrast, modern tall buildings in the United States are designed to achieve a probability of collapse of 10% or less under extreme shaking as characterized by the risk-targeted maximum considered earthquake (MCE_R) (often associated with a 2475-year return period, those this varies by location).

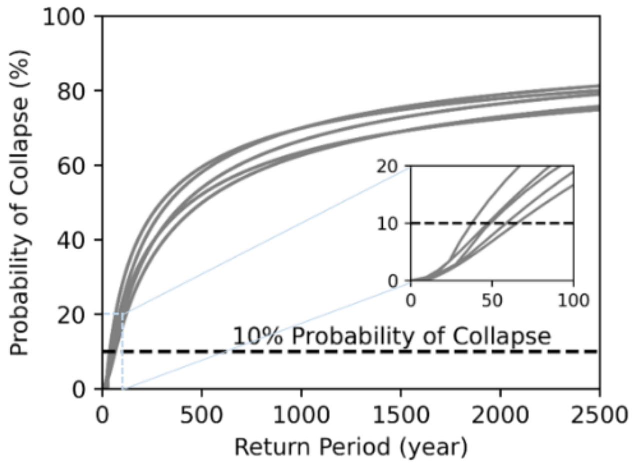

Figure 6: Collapse fragility functions of five 10-story archetypes. Black dashed line indicates a 10% probability of collapse.

CONCLUSIONS

A suite of five 10-story archetype non ductile reinforced concrete shear wall buildings are used in this study to develop robust structural analysis models to explore the variability in collapse risk of this taxonomy of buildings. Archetypes were selected based on an existing database of such buildings in the City of Vancouver. Three-dimensional fiber-based nonlinear structural analysis models were developed to the assess seismic performance of these buildings under ground motion suites representative of four distinct hazard levels (return period of 100, 475, 975, and 2475-year) and the three distinct tectonic regimes (crustal, inslab, and interface earthquakes). This multiple stripe analysis is used to quantify collapse at each shaking intensity. Collapse fragility functions are then derived by fitting a lognormal distribution using the maximum likelihood estimator. Furthermore, the annualized and 50-year collapse risk of each archetype is evaluated by integrating the collapse fragility with the corresponding seismic hazard curve.

The results of this study highlight high levels of collapse risk in these older non-ductile reinforced concrete shear wall buildings, particularly when compared to those in modern buildings. The 50-year collapse risk estimates in these older non-ductile RCSW buildings range from 26.6% to 35.3%, in huge contrast with the 1% in 50-year collapse risk in modern building codes.

This work is expanded by including a larger set of archetypes to explore the variation in collapse risk across different heights. The outcomes of the expanded project will enable characterizing the seismic performance of these high-risk driving buildings in a regional seismic risk model in a robust way and thereby providing a context for risk-informed decision making. Details of the expanded part of this work are forthcoming [12].

ACKNOWLEDGMENTS

This research was funded by Canada's Natural Sciences and Engineering Research Council under Discovery Grant No. RGPIN-2019-04599, as well as Canada's New Frontiers in Research Fund – Exploration under Grant No. NFRFE-2018-01060. The authors also appreciate Jack Chen, Professor Perry Adebar, and Professor Ken Elwood for developing and sharing the building inventory for this study. The authors would also like to acknowledge contributions from Jack Chen (former UBC student) in developing the OpenSeesPy models.

REFERENCES

[1] Molina Hutt C, Almufti I, Willford M, et al. Seismic Loss and Downtime Assessment of Existing Tall Steel-Framed Buildings and Strategies for Increased Resilience. *J Struct Eng U S* 2016; 142: 1–17.

[2] Molina Hutt C, Rossetto T, Deierlein GG. Comparative risk-based seismic assessment of 1970s vs modern tall steel moment frames. *J Constr Steel Res* 2019; 159: 598–610.

[3] Adebar P, Devall R, Mutrie J. Evolution of high-rise buildings in Vancouver, Canada. *Struct Eng Int* 2017; 27: 7–14.

[4] Canadian Standards Association (CSA). A23.3 - Design of concrete structures.

[5] NRC. National Building Code of Canada.

[6] Yathon J, Adebar P, Elwood KJ. A detailed inventory of Non-ductile concrete shear wall buildings. *Earthq Spectra* 2017; 33: 605–622.

[7] Jünemann R, de la Llera JC, Hube MA, et al. Study of the damage of reinforced concrete shear walls during the 2010 Chile earthquake: Study of Damage of RC Shear Walls during the 2010 Chile Earthquake. *Earthq Eng Struct Dyn* 2016; 45: 1621–1641.

[8] Wallace JW, Massone LM, Bonelli P, et al. Damage and Implications for Seismic Design of RC Structural Wall Buildings. *Earthq Spectra* 2012; 28: 281–299.

[9] Kam WY, Pampanin S, Elwood K. Seismic performance of reinforced concrete buildings in the 22 February Christchurch (Lyttelton) earthquake. *Bull N Z Soc Earthq Eng* 2011; 44: 239–278.

[10] Birley AC. Seismic Performance of Slender Reinforced Concrete Structural Walls. University of Washington, 2012.

[11] Abdullah SA, Wallace JW. Drift Capacity at Axial Failure of RC Structural Walls and Wall Piers. *J Struct Eng* 2021; 147: 04021062.

[12] Kakoty P, Molina Hutt C, Elwood KJ. Quantifying Variability in the Collapse Risk of Tall Non-Ductile Reinforced Concrete Shear Wall Buildings. (In-Preparation)

[13] Gogus A, Asce M, Wallace JW, et al. Seismic Safety Evaluation of Reinforced Concrete Walls through FEMA P695 Methodology. 2015; 141: 1–17.

[14] Marafi NA, Ahmed KA, Lehman DE, et al. Variability in Seismic Collapse Probabilities of Solid- and Coupled-Wall Buildings. *J Struct Eng* 2019; 145: 04019047.

[15] Pugh JS, Lowes LN, Lehman DE. Nonlinear line-element modeling of flexural reinforced concrete walls. *Eng Struct* 2015; 104: 174–192.

[16] Pugh JS, Lowes LN, Lehman DE. Accurate Methods for Elastic Seismic Demand Analysis of Reinforced Concrete Walled Buildings. *J Struct Eng* 2017; 143: 04017062.

[17] Eksir Monfared A, Molina Hutt C, Kakoty P, et al. Effects of the Georgia Sedimentary Basin on the Response of Modern Tall RC Shear-Wall Buildings to M9 Cascadia Subduction Zone Earthquakes. *J Struct Eng* 2021; 147: 05021003.

[18] Zhu M, McKenna F, Scott MH. OpenSeesPy: Python library for the OpenSees finite element framework. *SoftwareX*. Epub ahead of print 2018. DOI: 10.1016/j.softx.2017.10.009.

[19] Scott MH. A Tale of Two Element Formulations, https://portwooddigital.com/2020/02/23/a-tale-of-two-element-formulations/ (2020, accessed 10 April 2023).

[20] Mohd Yassin MH. *Nonlinear analysis of prestressed concrete structures under monotonic and cyclic loads*. Ph.D., University of California, Berkeley, https://www.proquest.com/docview/304097673/abstract/3FEAE13E80754E1APQ/1 (accessed 11 April 2023).

[21] Hognestad E. Study of combined bending and axial load in reinforced concrete members.

[22] Menegotto M, Pinto PE. Method of analysis for cyclically loaded reinforced concrete plane frames including changes in geometry and non-elastic behavior of elements under combined normal force and bending. Zurich, Switzerland, 1973.

[23] Zhang T. *Seismic Assessment of Singly Reinforced Concrete Walls in Pre-1970s Multi-Storey Buildings*. University of Auckland, 2020.

[24] NZS 1900:1964. Model Building Bylaw: Basic Design Loads and Commentary.

[25] Wallace JW, Elwood KJ, Massone LM. Investigation of the Axial Load Capacity for Lightly Reinforced Wall Piers. *J Struct Eng* 2008; 134: 1548–1557.

[26] Jalayer F. *Direct Probabilistic Seismic Analysis: Implementation Non-Linear Dynamic Assessments*. Stanford University, 2003.

[27] NRC. *National Building Code of Canada*. Ottawa: National Research Council Canada, 2020.

[28] Baker JW. Efficient Analytical Fragility Function Fitting Using Dynamic Structural Analysis. *Earthq Spectra* 2015; 31: 579–599.

[29] Kakoty P, Dyaga SM, Molina Hutt C. Impacts of simulated M9 Cascadia Subduction Zone earthquakes considering amplifications due to the Georgia sedimentary basin on reinforced concrete shear wall buildings. *Earthq Eng Struct Dyn* 2021; 50: 237–256.

[30] Liel AB, Haselton CB, Deierlein GG. Seismic Collapse Safety of Reinforced Concrete Buildings. II: Comparative Assessment of Nonductile and Ductile Moment Frames. *J Struct Eng* 2011; 137: 492–502.